

Dynamic light scattering from semidilute cellulose-tri-carbanilate solutions

Markus Wenzel, Walther Burchard and Klaus Schätzel*

Institute of Macromolecular Chemistry, University of Freiburg, Stefan-Meier-Strasse 31, FRG

(Received 8 July 1985; revised 2 September 1985)

A series of cellulose-tri-carbanilates (CTC) with a range of $M_w = 130\,000$ to $1\,000\,000$ has been studied in dioxane at 20°C by static and dynamic light scattering. CTC is a semiflexible chain with a persistence length of 110 \AA . In two cases ($M_w = 130\,000$ and $1\,000\,000$) a concentration region from dilute to $20c^*$ was covered, where $c^* = 1/|\eta|$ is taken as the coil overlap concentration. Up to $3c^*$ usual dilute solution behaviour was found. At about $3c^*$ a sharp decrease in $1/M_{\text{app}} [= Kc/R(q=0)]$ and in the apparent diffusion coefficient $D(c)$ (determined from the first cumulant of the time correlation function (TCF)) was observed. Simultaneously, the mean square radius of gyration increases. Analysis of the TCF reveals two modes of motion: the mode which is fast, increases with c with an exponent of about 1.0 ± 0.1 and may be attributed to the cooperative diffusion coefficient of an entangled network. The other, which is slow, decreases with an exponent of about -2.6 ± 0.2 and thus is appreciably larger in value than -1.75 which is predicted for the self-diffusion of single chains. Master curves are obtained for M/M_{app} and $D(c)/D_0$ as function of c/c^* . The observed behaviour indicates that there is no transient network formation. The results are, however, consistent with a model of entangled clusters existing in the region $c^* \leq c \leq 10c^*$.

(Keywords: dynamic light scattering; cellulose-tri-carbanilate; semidilute solution; cooperative diffusion; slow modes of motion)

INTRODUCTION

Cellulose derivatives are known as fairly stiff chain molecules, and it is mainly this property which makes these polymers interesting for principal reasons as well as for application. Among other cellulose derivatives¹, the solution properties of cellulose-tri-carbanilates (CTC) have been studied extensively in previous papers²⁻⁹. Most of the investigations have been carried out in dioxane at room temperature. A persistence length of $a = 110\text{ \AA}$ was found by small-angle neutron scattering⁷, by flow birefringence⁶ and from the molecular weight dependence of the radius of gyration^{4,9}. This persistence length corresponds to a characteristic ratio of $C_\infty = 2a/l = 42.7$, where $l = 5.15^{10}$ is the virtual bond length of a β -glucose in cellulose. Cellulose itself dissolved in complexing solvents is not really a stiff molecule but with $C_\infty = 9.5^1$ it exhibits the same rotational freedom as synthetic flexible chain molecules. The rigidity of the cellulose derivatives are caused by bulky substituents. The structure of CTC is given in *Figure 1*.

Dioxane is a good solvent for CTC but up to now only the dilute solution behaviour has been studied. Recent investigation of more concentrated, semidilute solutions have aroused much interest¹³ mainly because of their dynamic properties¹⁴⁻¹⁶. In semidilute solutions the coils of different macromolecules are at a stage of overlapping segments and therefore the individual molecules cannot be observed any longer. Instead a cooperative behaviour is observed¹³.

For flexible chain molecules de Gennes and his coworkers have developed a simple picture for the structure of these solutions. According to this picture a

transient network of interpenetrating and entangled chains is formed. The behaviour is described by the correlation length ξ (which is the average distance between two points of entanglement) and the overlap concentration c^* , which appears as a scaling factor in the theory. The predictions by de Gennes are valid at concentrations much larger than the c^* , but for the cross over region around $c \simeq c^*$ no definite predictions can be made.

Recently we have reported dynamic and static light scattering measurements on poly(vinylpyrrolidone) (PVP) in aqueous solution up to a concentration of $6c^*$.¹⁹ PVP is a flexible chain molecule ($C_\infty = 7.6^{20}$) which is readily soluble in water, various alcohols and a large number of common organic solvents. Near c^* a sharp increase in the apparent mean square radius of gyration $\langle S^2 \rangle_c^{21}$ was observed. Simultaneously the time correlation function of scattered light clearly exhibited two modes of motion: a fast, gel-like diffusion with a coefficient D_{coop} , which increases with c , and a slow one with the coefficient D_{slow} , which was difficult to assign to a self-diffusion of individual chains¹⁹.

The purpose of the present paper is the study of these phenomena with a different chain covering a wider region of concentrations. It is of interest whether or not a behaviour similar to PVP would be found with CTC, and if so, what influence a certain chain stiffness would have on the solution properties.

EXPERIMENTAL

Sample preparation

Samples were prepared either from Temmings Linters by direct carbanilation or from a cellulose 2-1/2 acetate

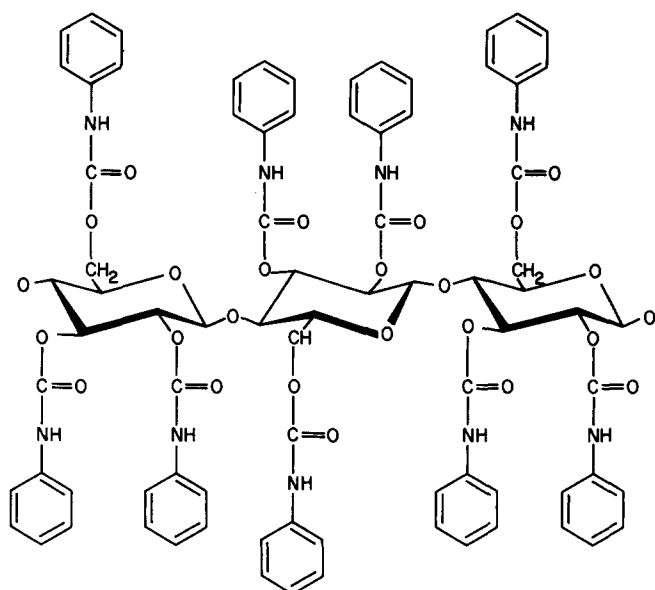


Figure 1 Chemical structure of cellulose-tri-carbanilate (CTC). Molecular weight of the monomer unit $M_0 = 519$

(Rhodia) which was saponified with concentrated NH_3 solution prior to carbanilation.

To prepare the derivatives the dried cellulose was immersed in pyridine (at least 4 times the weight of the cellulose) and heated under an inert atmosphere to 100°C . Twice the stoichiometric amount of phenylisocyanate was added with stirring and the reaction mixture was left stirring for 4 to 8 h. The highly viscous solution was precipitated in methanol and washed several times with methanol. After redissolving the material in dioxane the solution was centrifuged for 30 min in a Beckmann fixed angle rotor at 25000 rpm. The clear solution was precipitated in water and dried over P_2O_5 . Nitrogen content: theor. 8.08%; found 7.99 to 8.1%.

Fractionation

The samples were fractionated by adding water to a 0.5% CTC solution in acetone. The obtained mixture was warmed in a water bath until a homogeneous solution was obtained. With stirring, the solution was slowly cooled to room temperature and a gel-like fraction was obtained.

Gel permeation chromatography

The molecular weight distributions were measured by gel permeation chromatography (g.p.c.) in THF. The calibration curve shown in Figure 2 was obtained by an iteration procedure. To a first approximation the weight average molecular weight of the fractions were taken and M_n was calculated using this calibration curve. The mean $(M_n/M_w)^{1/2}$ was taken then for the second approximation. This calibration curve gave the correct M_w -values for the low molecular weight products but too large M_w -values for the high molecular weights. The calibration curve was then varied in a trial/error procedure until the calculated M_w coincided with M_w from the light scattering. The data for M_w , M_n and the resulting polydispersities are given in Table 1.

Light scattering

Molecular weights M_w and diffusion coefficients D_z were measured in dioxane at 20°C by combined static and dynamic light scattering with an instrument that is

described elsewhere²³. M_w , $\langle S^2 \rangle_z$, A_2 , D_z and the coefficient k_D of the concentration dependence of $D(c)$ were evaluated from static and dynamic Zimm plots. Figure 3 gives an example. The required parameters are given in Table 2.

Autocorrelator/structurator

For the detection of the time correlation function (TCF) a special 4×4 bit autocorrelator/structurator from the ALV Langen company was used²⁴. This correlator allows determination of the TCF at equally spaced delay times ('single tau mode') or at quasi-logarithmically spaced delay times ('multiple tau mode'). In the single tau mode up to 1024 channels are used for the calculation of the TCF; an extra delay of arbitrary length and at an arbitrary position can be inserted for determining the base line.

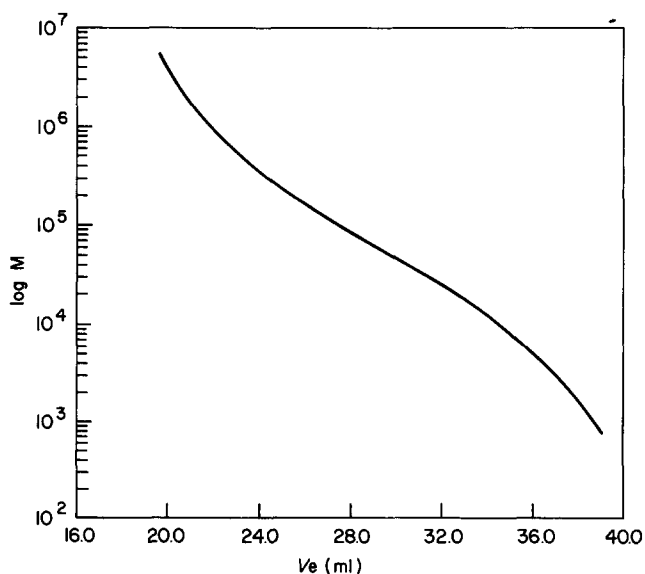


Figure 2 Gel permeation chromatography calibration curve for CTC in THF

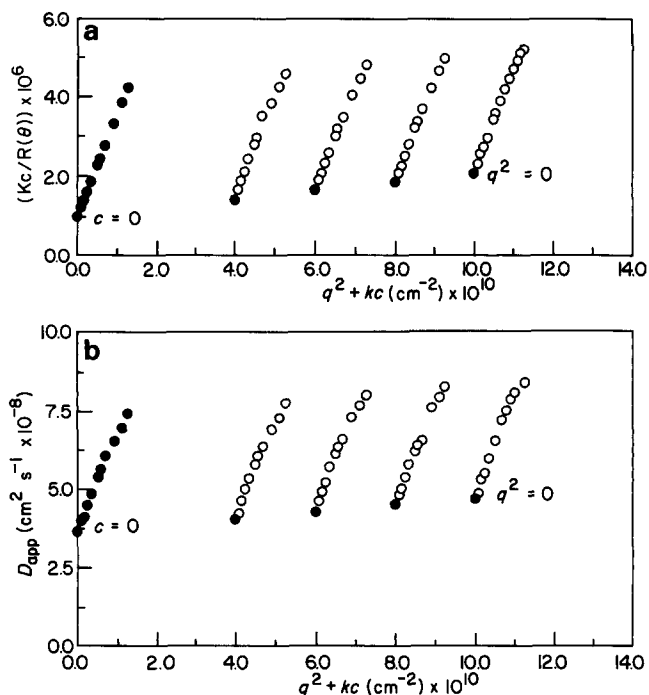


Figure 3 (a) Static and (b) dynamic Zimm plots of the light scattering measurements from CTC-5 in dioxane at 20°C

Table 1 Molecular weights M_w (g.p.c.) and M_n (g.p.c.) according to gel permeation chromatography and the resulting polydispersity M_w/M_n compared with M_w (LS) obtained from light scattering

Sample	M_w (LS)	M_w (g.p.c.)	M_n (g.p.c.)	M_w/M_n
CTC-1	131 000	159 000	130 000	1.22
CTC-2	200 000	236 000	192 000	1.23
CTC-3	426 000	486 000	288 000	1.69
CTC-4	741 000	866 000	610 000	1.42
CTC-5	1 000 000	1 070 000	644 000	1.67

Table 2 List of the solvent refractive index n , the refractive index increment dn/dc and of the solvent viscosity η_0 (dioxane) at 20°C, and for the applied wavelength of the blue line of an Argon ion laser

λ_0	n	dn/dc	η_0
488 nm	1.428	0.156	1.26 cP

In the multiple tau mode the first 16 channels are equally spaced in time. For the next group of 8 channels, pairs of adjacent samples are added and correlation channels with doubled delay time increments and doubled width of sampling intervals are computed. The same doubling procedure is repeated after every 8 channels and provides temporal correlation estimates over a large lag time range with optimum signal-to-noise performance^{24a}. A total of 10 groups provide 88 channels with a lag time spacing over a range of almost 1:8000. The shortest available lag time is 20 ns, input count rates may range up to 100 MHz.

Overflows of the 4-bit data format due to the addition of adjacent samples are avoided by optional addition of a random bit and division by two between subsequent groups of channels. This 'random preset scaling', which is also available to reduce very high input count rates prior to processing, avoids bias and distortion of the correlogram^{24b,c}. All stages, remaining overflows of the 4-bit format are automatically detected and flagged to enable a correct choice of the scaling level.

RESULTS

A series of cellulose-tri-carbanilates (CTC) in the range of $M_w = 130\,000$ – $1\,000\,000$ was studied in dioxane at 20°C by static and quasi-elastic light scattering. In two cases, i.e. CTC-1 ($M_w = 130\,000$) and CTC-5 ($M_w = 1\,000\,000$) a concentration region from dilute to $20c^*$ was covered, where $c^* = 1/|\eta|$ is set as the coil-overlap concentration.

Dilute solution properties

In dilute solution CTC displays the usual behaviour. It was possible to determine M_w , A_2 , $\langle S^2 \rangle$, D_z in good agreement with earlier measurements carried out with different instruments^{3,4,8,22}. $\langle S^2 \rangle_z$ and D_z can be described by exponential equations, though the exponents are a little higher than for flexible chains (Figures 4 to 6). The persistence length a and the characteristic ratio C_∞ were obtained from diffusion measurements by applying the Cowie-Bywater plot²⁵, which is shown in Figure 7. This plot is based on the equation

$$kT/\eta_0 D_z M_w^{1/2} = P_0 A + 0.201(P_0/A^2) B M_w^{1/2} \quad (1)$$

where

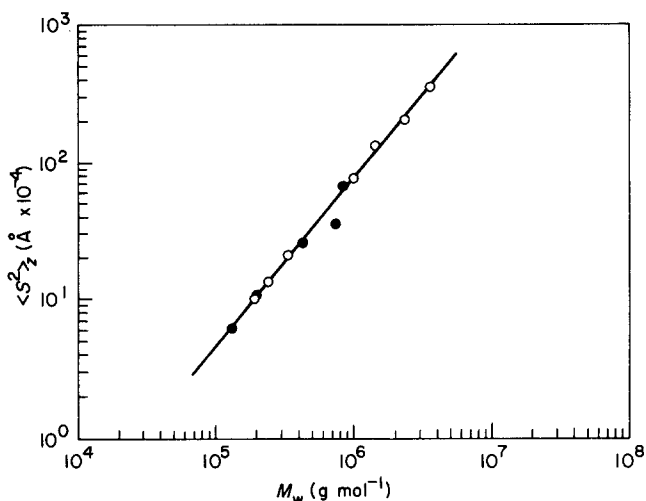
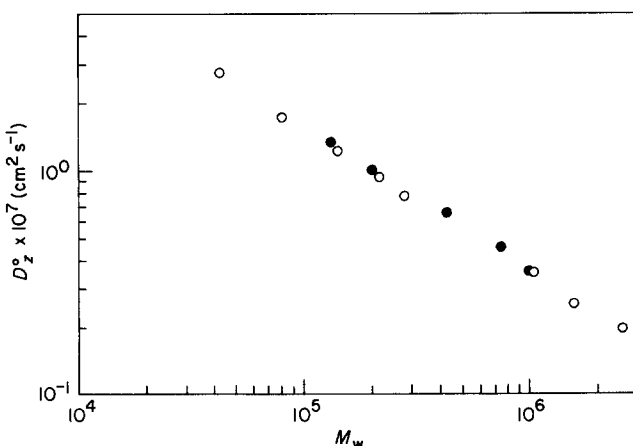
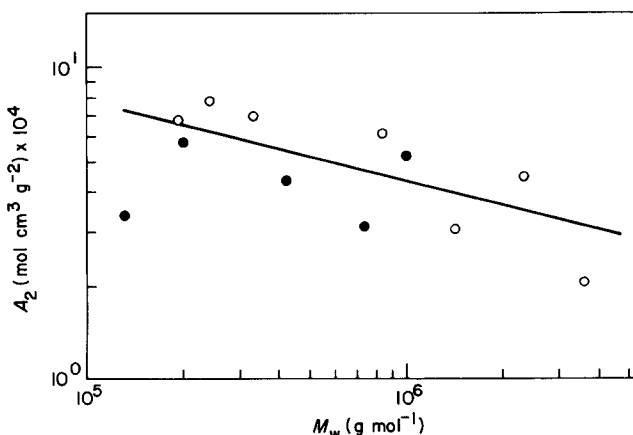
$$A = [6\langle S^2 \rangle_0/M]^{1/2} \quad (2)$$

The characteristic ratio C and the persistence length a are given then by

$$C_\infty = 6\langle S^2 \rangle_0/Nl^2 = A^2 M_0/l^2 \quad (3)$$

and

$$a = C_\infty l/2 \quad (4)$$


Figure 4 Molecular weight dependence of the mean square radius of gyration in dioxane at 20°C. (—●—) this work; (—○—) refs. 3 and 4

Figure 5 Molecular weight dependence of the translational diffusion coefficient D_z of CTC in dioxane at 20°C. (—●—) this work, (—○—) ref. 8

Figure 6 Molecular weight dependence of the second virial coefficient A_2 of CTC in dioxane at 20°C. (—●—) this work, (—○—) ref. 3

where $M_0 = 519$ is the repeating unit molecular weight and $l = 5.15 \text{ \AA}$ its length.

The results are collected in Table 3 and the molecular weight dependences of A_z , $\langle S^2 \rangle_z$ and D_z are shown in Figures 4 to 6. The persistence length has a value of 65.7 \AA and the characteristic ratio C_∞ is 25.6.

Semidilute solutions

For higher concentrations normal behaviour is observed only up to a concentration of about $3c^*$. In this region $D(c)$ increases with c , $\langle S^2 \rangle_c$ remains nearly constant²¹ and $1/M_{app}$ increases as the result of the repulsive polymer-polymer interaction. Above $3c^*$ a sharp decrease in $1/M_{app} = Kc/R(q=0)$, and in the apparent diffusion coefficient $D(c)$ (determined from the first cumulant of the time correlation function of the scattered electric field (TCF)) is observed. Simultaneously the apparent mean square radius of gyration $\langle S^2 \rangle_c$ ²¹ increases. To answer the question whether two modes of motion really exist in more concentrated solutions, the TCF was registered at two different sample times. Applying the CONTIN program by Provencher²⁶, two relaxations and the corresponding apparent diffusion coefficients were obtained. In most cases the values depend on the scattering angle. Therefore extrapolation towards $q=0$ was carried out which yielded $D(c)_{fast}$ and $D(c)_{slow}$.

The following Figures 8a-c show double logarithmic plots of $\langle S^2 \rangle_c$, $D(c)/D_0$, $D(c)_{fast}/D_0$, $D(c)_{slow}/D_0$ and M_w/M_{app} against c/c^* . These quantities can be approximated by the following exponential equation

$$\langle S^2 \rangle_c \sim (c/c^*)^{a_s} \tag{5a}$$

$$D(c)_{fast} = (c/c^*)^{a_{fast}} \tag{5b}$$

$$D(c)_{slow} \sim (c/c^*)^{a_{slow}} \tag{5c}$$

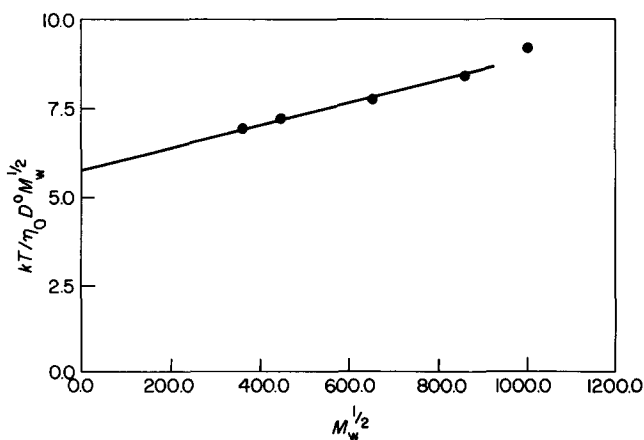


Figure 7 Cowie-Bywater plot for CTC in dioxane at 20°C for deriving the unperturbed chain dimensions

Table 3 List of the dilute solution properties

Sample	M_w	$A_z \times 10^{-4}$ (mol cm ³ /g)	$\langle S^2 \rangle_z \times 10^2$ (nm ²)	$D_z \times 10^{-7}$ (cm ² /s)	$R_{h,z}$ (nm)	ρ
CTC-1	131 000	3.38	6.2	1.37	12.27	2.03
CTC-2	200 000	5.75	10.7	1.03	16.39	2.00
CTC-3	426 000	4.38	27.7	0.664	25.67	2.05
CTC-4	741 000	3.13	36.1	0.465	36.66	1.64
CTC-5	1 000 000	5.25	78.00	0.365	46.70	1.89

$$D_{cum}/D_0 \sim (c/c^*)^{a_{cum}} \tag{5d}$$

$$M(0)/M_{app} \sim (c/c^*)^{a_M} \tag{5e}$$

where $M(0)$ and D_0 are the molecular weight and the diffusion coefficient of the sample at zero concentration, respectively, and M_{app} is the apparent particle weight which by definition is given by

$$Kc/R(q) = 1/M_{app} = 1/M(c) + 2A_2c + 3A_3c^2 + \dots \tag{6}$$

The exponents are listed in Table 4.

Figure 9 shows as an example typical TCF's for a few concentrations, where for practical reason a plot of $g_1(t)$ against $\log t$ was chosen.

DISCUSSION

Before discussing the results it will be useful to recall the picture of the dilute and semidilute solutions.

Dilute solutions

In dilute solutions individual molecules are observed. In good solvents they interact like hard spheres. The measured properties are the result of a combination of thermodynamic and hydrodynamic interactions, and the molecular properties are obtained after extrapolation to zero concentration. The results described in this paper are in remarkably good agreement with data from earlier measurements, even for the diffusion coefficient published many years ago^{3,4,8}. This last result is not selfevident since in the earlier measurements the boundary-spreading-technique was applied, while in the present case the diffusion coefficient was determined from the Brownian motion without applying an external force. In the first case the weight average and in the second the z-average of the diffusion coefficient is obtained. The good agreement is on one hand a proof for the Stokes-Einstein law

$$D_z = kT/(6\pi\eta_0 R_h)_z \tag{7}$$

and on the other hand, it indicates a fairly narrow distribution of the samples. Since CTC forms a random coil, the hydrodynamic radius R_h corresponds to an effective hydrodynamic sphere radius which needs not have the same value as the radius of gyration. A measure for the difference of these two molecular parameters is given by the factor $\rho = \langle S^2 \rangle^{1/2}/R_h$. According to Benmouna and Akcasu²⁷ this parameter is given by the following equation

$$\rho(v) = 6/\{1-v\}(2-v)[3\pi(1+v)(1+2v)]^{1/2} \tag{8}$$

where v is the exponent of the molecular weight dependence of the radius of gyration. A value of $v = 0.6$ has

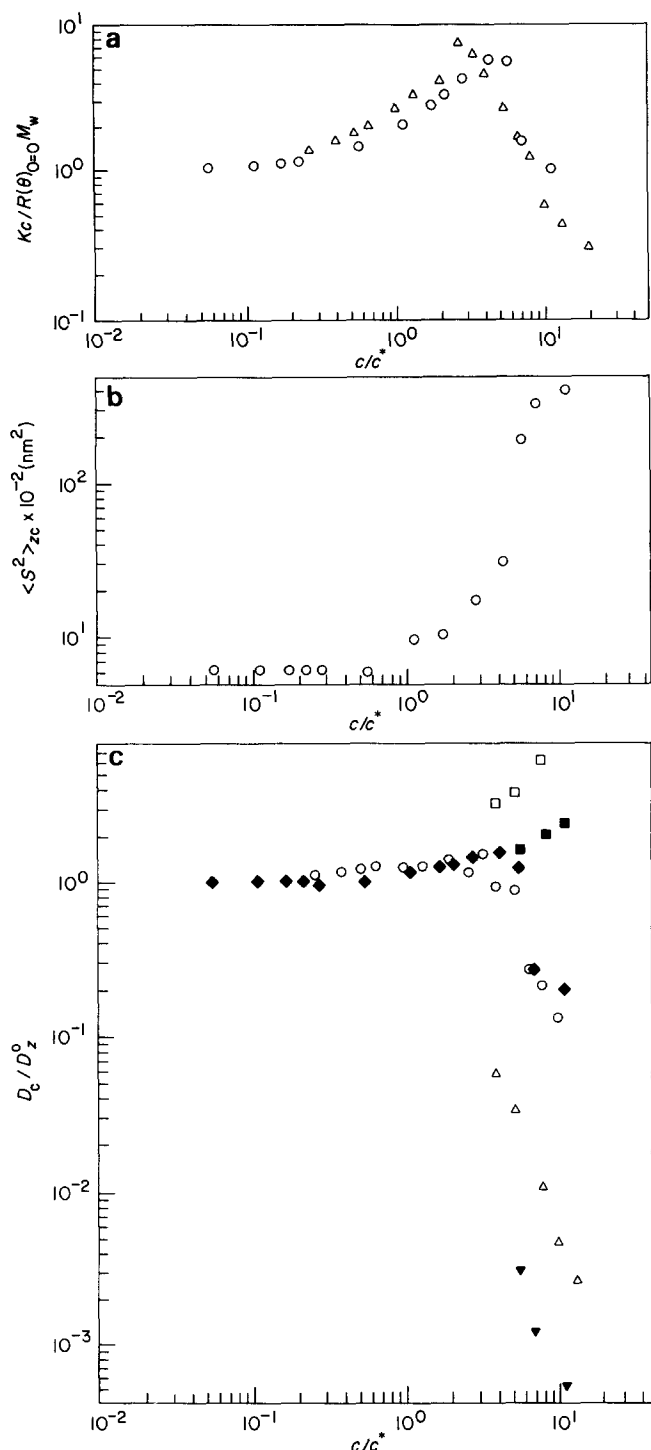


Figure 8 Results from the combined static and dynamic light scattering measurements from CTC in semidilute solutions. All data are plotted against c/c^* where $c^* = 1/[\eta]$ was set. (a) Concentration dependence of $(Kc/R(q=0))M_w = M_w/M_{app}$; (b) concentration dependence of the apparent particle mean square radius of gyration²¹; (c) concentration dependence of the various diffusion coefficients normalized with respect to the zero concentration translational diffusion coefficient. (i) (○) and (●): D_{cum}/D_0 where D_{cum} was determined from the first cumulant of the time correlation function (TCF). (ii) and (■): D_{fast}/D_0 where D_{fast} is the faster component in the TCF. (iii) (△) and (▼): D_{slow}/D_0 where D_{slow} is the slow component in the TCF. The filled symbols correspond to $M_w = 130\,000$ and the open symbols to $M_w = 1\,000\,000$

been found which gives, for monodisperse samples, a theoretical value of $\rho_{th} = 1.86$. Polydispersity increases the factor slightly and for $M_w/M_n = 1.45 \pm 0.2$ a value of $\rho = 2.05 \pm 0.1$ is predicted. The experimental data shown in Table 3 lie in this spread of error.

The unperturbed dimensions and the persistence length, as determined from the Cowie-Bywater plot, appear to be too low compared with other measurements⁹. There is in fact ambiguity concerning the amplitude factor P_0 , which on the basis of the Kirkwood-Riseman theory is 5.2. However, in theta solvents a hydrodynamic radius was found²⁸ 18% higher than predicted by this theory and this implies an increase to $P_0 = 6.1$ and using this P_0 value, the results in Table 4 are obtained. The value of $a = 47 \text{ \AA}$ is much smaller than the 110 \AA found by other techniques^{4,7,9}. The difference may result from the existing chain stiffness which has a noticeable effect on the diffusion coefficient of the low molecular weight compounds and which makes the application of the Cowie-Bywater plot no longer reliable.

Semidilute solutions

If the concentration increases beyond c^* , a stage is reached where the coils start to overlap and therefore motion of individual chains will no longer be observed. According to de Gennes a transient network of entangled chains is formed for $c \gg c^*$. Des Cloiseaux²⁹ predicts a power law for the osmotic pressure given by the following equation

$$\pi/RT = (c/M)(c/c^*)^{1.25} \sim c^{2.25} \quad (9)$$

Table 4 List of exponents according to equations (5a) to (5c)

Sample	a_s	a_{fast}	a_{slow}	a_{cum}	a_M
CTC-1	1.82	1.1	-2.78	-2.63	-2.43
CTC-5	1.67	1.0	-2.59	-2.63	-2.43

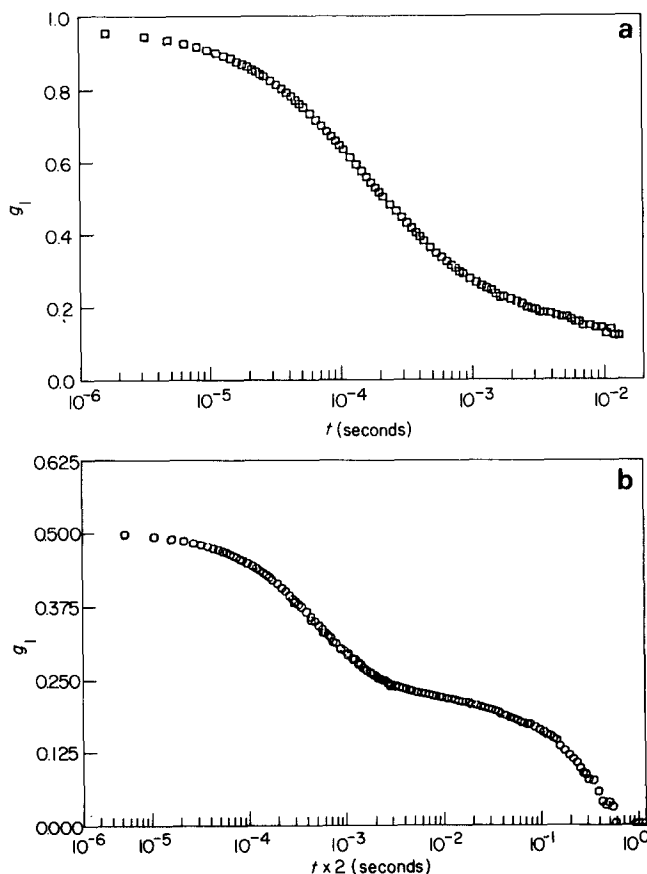


Figure 9 Two typical TCFs for CTC-5. (a) $c < c^*$; (b) $c > c^*$. Two well separated modes of motion are observable in the latter case

which gives for the light scattering intensity $Kc/R_0 \sim c^{1.25}$, because the intensity is proportional to $\partial\pi/\partial c$.

Two relaxation modes are predicted in the semidilute regime by de Gennes^{13,30}: a slow mode, D_{self} , which is assigned to the reptation of a single chain through the network³⁰, and a fast mode, D_{coop} , caused by the 'respiration' of the network itself¹³. This faster diffusion is evidently a cooperative motion, which in the theory of semidilute solution is related to the correlation length ξ of a network. It is given by the equation

$$D_{\text{coop}} = kT/6\pi\eta_0\xi \quad (10)$$

Since, on the other hand, ξ is expressed in terms of c/c^* as

$$\xi = R(c/c^*)^{3/4} \quad (11)$$

with R being the end-to-end distance of the individual chain, one has

$$D_{\text{coop}} = D_0(c/c^*)^{3/4} \quad (12)$$

where use was made of equation (7).

The two predicted exponents in a plot of D_{coop}/D_0 against (c/c^*) and D_{self} are $a_{\text{coop}} = 0.75$ and $a_{\text{self}} = -1.75$, respectively.

In order to make the subsequent discussion on the static properties more clear we rewrite equation (6) as follows

$$M/M_{\text{app}} = (M(0)/M(c))(1 + 2A_2M(c)c + 3A_3M(c)c^2 + \dots) \quad (13)$$

where $M(c)$ and $M(0)$ are particle weights at concentration c and $c=0$, respectively.

This relationship shows explicitly that M_{app} may decrease because of the repulsive interaction among the individual coils, but M_{app} may also increase via $M(c)$ as function of c , since the molecules may form a larger structure by association or other mechanisms.

Up to $3c^*$ the expected increase of M/M_{app} is observed. However, it exhibits an exponent $a_{\text{Mlow}} = 0.9 \pm 0.1$ smaller than predicted by des Cloiseaux. At $3c^*$ this curve passes through a sharp maximum and decreases strongly with an exponent of -2.43 . We find it worth noticing that the data from the two samples with different molecular weights form a common curve if the reduced molecular weight is used. The maximum and the sharp increase was not expected or predicted by des Cloiseaux. The strong increase of M_{app} is inconsistent with the existence of a network but indicates the formation of clusters. This conclusion is confirmed by measurements of $\langle S^2 \rangle_c$.

To avoid confusion it may be emphasized that $\langle S^2 \rangle_c$ does not necessarily represent the mean square radius of gyration of the individual macromolecules that is found at low concentrations. $\langle S^2 \rangle_c$ is an apparent quantity which

is obtained from the initial slope in the q^2 dependence of the reciprocal scattering intensity that was measured at a certain concentration. For aggregating macromolecules, for instance, $\langle S^2 \rangle_c$ represents the mean square radius of gyration of the aggregate at that concentration.

This radius is still an apparent one and somewhat smaller than the geometric one, since it contains the influence of the excluded volume of these particles. This becomes evident when writing the Debye equation in full

$$Kc/R(q) = 1/M(c) + 2A_2c + 3A_3c^2 + (1/3)(\langle S^2 \rangle_{0c}/M(c))q^2 \quad (14)$$

from which we find

$$\begin{aligned} \langle S^2 \rangle_c &= (M_{\text{app}}/M(c)\langle S^2 \rangle_{0c}) \\ &= \langle S^2 \rangle_{0c}/(1 + 2A_2M(c) + 3A_3M(c)c^2 \dots) \end{aligned} \quad (15)$$

where M_{app} is given by equation (6) and $\langle S^2 \rangle_{0c}$ is the mean square radius of gyration without the excluded volume interaction effect.

For a network, on the other hand, which is completely characterized by its mesh size ξ , Edwards³¹ and de Gennes¹³ find

$$Kc/R(q) \sim (1 + \xi^2q^2)/g \quad (16)$$

where g is the number of segments in the volume spanned by one mesh. Hence the slope in a plot of $Kc/R(q)$ against q^2 yields the squared correlation length which should decrease with an exponent of $-9/16 = -0.56$. Experimentally, however, a strong increase is observed with a power of about 1.17 ± 0.1 , and this behaviour is consistent with the interpretation of cluster formation.

Concerning the modes of motion we find a steeper increase for the fast motion than predicted. The simultaneously appearing slow mode of motion decreases with an exponent of -2.68 , much stronger than for a reptating chain, where an exponent -1.75 is predicted.

Slow modes of motion have been observed already for a long time^{19,33-40} but the origin of this motion remained unclear, since only the dynamic properties have been considered. The simultaneously recorded static light scattering now gives clearer insight into the structure of the semidilute solution. The high exponent of -2.68 and the coincidence of the slow mode with the increase of the particle radius of gyration makes it appear unlikely that this motion is a reptating self diffusion. The results are consistent, on the other hand, with the interpretation that the movement of entangled clusters is through the solution strongly hindered^{19,39}.

The larger exponent for the fast mode, which is actually that of the cooperative diffusion of a network under θ conditions¹⁸, may result from the rigidity of the CTC chains. Chain rigidity reduces the number of possible intramolecular contacts and thus suppresses the excluded volume effect making the chain more similar to an unperturbed chain. On the other hand, following the derivation of de Gennes and Brochard^{13,18}, one finds for a general v the relationship

$$D_{\text{coop}} = kT6\pi\eta_0\xi = D_0(c/c^*)^{v/(3v-1)} \quad (17)$$

which yields with $v = 0.63$ an exponent of $a_{\text{fast}} = 0.71$ which now is lower than 0.75 for a flexible chain.

Table 5 Unperturbed dimension $A = (6\langle S^2 \rangle_0/M)^{1/2}$, characteristic ratio $C_\infty = 6\langle S^2 \rangle_0/Nl^2$ and persistence length a for CTC in dioxane at 20°C. The data were obtained from the intercept of the Cowie-Bywater plot (Figure 7) where $\rho = \langle S^2 \rangle_0^{1/2}/R_h = 1.27$ was used ($P_0 = 6.1$ in equation (1), $M_0 = 519$, $l = 5.15 \text{ \AA}$)

A	C_∞	a
0.97 \AA mol^{-1}	18.4	46.9 \AA

CONCLUSIONS

To date we have a clear picture on the behaviour of macromolecules in dilute solution and in the semi-dilute regime. In the dilute regime the macromolecules move as individuals while in the semidilute regime a transient network of entangled chains apparently exists. Up to now, a more or less instantaneous transition from the one state to the other has been assumed which implies a sudden change from the isolated chain behaviour to that of the strongly inhibited molecules in the transient network. Such expectation is, however, not sensible, because from analytical theories^{41,42} and computer simulations of network formation⁴³ it is well known that the pre-gel state consists of highly branched clusters which grow as the gel-point is approached. Indeed, the transition to the transient network will resemble very much the percolation picture with the difference, however, that in entangled networks no permanent or locally fixed crosslinks exist. Thus cluster formation of entangled chains could have been expected, and the observed results are at least consistent by this interpretation. Recently Ballodge and Tirrell³⁹ reported other examples where slow motions accompanied with an increase of the scattering intensity was found, but they also gave examples where these slow motions could not be detected. In none of the various systems studied by us was such sample-dependent behaviour observed^{19,44,45} but in all cases a very similar behaviour as described in this paper was found.

Our results are also in agreement with earlier findings by Dautzenberg^{46,47} who reported for polystyrene in benzene, at larger concentrations, a strong increase of the apparent particle dimensions. He did not determine the overlap concentration c^* but he showed that this behaviour occurred if the distance between the centres of mass of the various coils become smaller than the radius of gyration. The strength of the increase depends on the pretreatment of the solutions, i.e. the effect becomes less pronounced after a longer centrifugation of the solutions. This effect is presently studied more systematically and will be discussed elsewhere.

ACKNOWLEDGEMENTS

We are indebted to Dr M. Müller, Chemische Werke Hüls, Marl, for the preparation and fractionation of the samples. We also wish to thank Mr M. Eisele for his advice in handling the new autocorrelator/structurator. The work was kindly supported by the Deutsche Forschungsgemeinschaft within the scheme SFB 60.

REFERENCES

- 1 Brandrup, J. and Immergut, E. H. (Eds.) 'Polymer Handbook', Wiley, New York, 1975
- 2 Burchard, W. *Z. Phys. Chem.* 1964, **42**, 293
- 3 Burchard, W. *Makromol. Chem.* 1965, **88**, 11
- 4 Burchard, W. *Br. Polym. J.* 1971, **23**, 214
- 5 Gupta, A. K., Marchal, E. and Burchard, W. *Macromolecules* 1975, **8**, 843
- 6 Nordermeer, J. W. M., Daryanani, R. and Janeschitz-Kriegl, H. *Polymer* 1975, **16**, 359

- 7 Gupta, A. K., Cotton, J. P., Marchal, E., Burchard, W. and Benoit, H. *Polymer* 1976, **17**, 363
- 8 Sutter, W. and Burchard, W. *Makromol. Chem.* 1978, **179**, 1961
- 9 Hsu, B., McWherter, C. A., Brant, D. A. and Burchard, W. *Macromolecules* 1982, **15**, 1350
- 10 In the crystalline state CTC forms a left handed three-fold (3_2) helix^{11,12} with a pitch height per repeating unit of $h=5.0$ Å; for the zig-zag chain conformation the length is 5.15 Å. In solution a value between these two limits may be expected
- 11 Zugenmaier, P. *J. Appl. Polym. Sci.* 1983, **37**, 223
- 12 Zugenmaier, P. in 'Polysaccharide' (Ed. W. Burchard), Springer-Verlag, Heidelberg, 1985, p. 260
- 13 de Gennes, P.-G. 'Scaling Concepts in Polymer Physics', Cornell University Press, Ithaca, New York, 1979
- 14 Candau, S. J., Bastide, J. and Delsanti, M. *Adv. Polym. Sci.* 1982, **44**, 27
- 15 Munch, P. J. *et al. J. Phys. (Paris)* 1977, **38**, 971
- 16 Burchard, W. *Chimica* 1985, **39**, 1
- 17 Tanaka, T., Hocker, L. and Benedek, G. B. *J. Chem. Phys.* 1973, **59**, 515
- 18 Brochard, F. and de Gennes, P.-G. *Macromolecules* 1977, **10**, 1157
- 19 Eisele, M. and Burchard, W. (a) *Pure Appl. Chem.* 1984, **56**, 1379; (b) *Macromolecules* 1984, **17**, 1636
- 20 (a) Burchard, W. 'Habilitationsschrift', Freiburg 1965; (b) Eisele, M. *Diploma Thesis*, Freiburg, 1984
- 21 $\langle S^2 \rangle_c$ is not necessarily the mean square radius of gyration of an individual molecule. It is determined from the initial slope of $Kc/R(q)$ as function of q^2 in the usual manner
- 22 Burchard, W. and Husemann, E. *Makromol. Chem.* 1961, **44-46**, 358
- 23 Bantle, S., Schmidt, M. and Burchard, W. *Macromolecules* 1982, **15**, 1604
- 24 ALV-3000 Correlator/Structurator, supplied by ALV-Langen/Hessen, FRG
- 24 (a) Schätzel, K. in 'Proc. 6th Intl. Conf. on Photon Correlation and other Optical Techniques in Fluid Mechanics', Cambridge, 1985; (b) Schätzel, K. *Appl. Phys.* 1980, **22**, 251; (c) Schätzel, K. in 'Photon Correlation Techniques in Fluid Mechanics', Springer, Berlin, 1983, p. 226
- 25 Cowie, J. M. G. and Bywater, S. *Polymer* 1960, **6**, 197
- 26 Provencher, S. W. *Biophys. J.* 1976, **16**, 27
- 27 Ackasu, A. Z. and Benmouna, M. *Macromolecules* 1978, **11**, 1187
- 28 Schmidt, M. and Burchard, W. *Macromolecules* 1981, **14**, 210
- 29 des Cloiseaux, J. *J. Phys. (Paris)* 1975, **36**, 281
- 30 de Gennes, P.-G. *Nature (London)* 1979, **282**, 367
- 31 Edwards, S. F. *Proc. Roy. Soc. (London)* 1966, **88**, 265
- 32 Burchard, W., Schmidt, M. and Stockmayer, W. H. *Macromolecules* 1980, **13**, 1265
- 33 Nose, T. and Chu, B. *Macromolecules* 1979, **12**, 590
- 34 Chu, B. and Nose, T. (a) *Macromolecules* 1979, **12**, 599; (b) *Macromolecules* 1980, **13**, 122
- 35 Mathiez, G., Weisbuch, G. and Mouttet, G. *Biopolymers* 1979, **18**, 1463
- 36 (a) Amis, E. J., Janmey, P. A., Ferry, J. D. and Yu, H. *Polym. Bull.* 1981, **6**, 13; (b) Amis *et al. Macromolecules* 1983, **16**, 44; (c) Amis, E. J. and Han, C. C. *Polymer* 1982, **23**, 1403; (d) Amis, E. J., Han, C. C. and Matsushita, Y. *Polymer* 1984, **25**, 650
- 37 (a) Brown, W., Johnsen, R. M. and Stilbs, P. *Polym. Bull.* 1983, **9**, 305; (b) Brown, W., Stilbs, P. and Johnsen, R. M. *J. Polym. Sci., Polym. Phys. Edn.* 1980, **20**, 1771; (c) Brown, W. *Macromolecules* 1984, **17**, 66
- 38 Candau, S. J., Butler, I. and King, T. A. *Polymer* 1983, **24**, 1601
- 39 Ballodge, S. and Tirrell, M. *Macromolecules* 1985, **18**, 819
- 40 Selzer, J. C. *J. Chem. Phys.* 1983, **79**, 1044
- 41 Flory, P. J. 'Principles of Polymer Chemistry', Cornell University Press, Ithaca, New York, 1953
- 42 Stockmayer, W. H. (a) *J. Chem. Phys.* 1943, **11**, 45; (b) *J. Chem. Phys.* 1944, **12**, 125
- 43 (a) Stauffer, D. *Pure Appl. Chem.* 1981, **53**, 1476; (b) Stauffer, D. *Phys. Reports* 1979, **54**, 1; (c) Stauffer, D., Coniglio, A. and Adam, M. *Adv. Polym. Sci.* 1982, **44**, 105
- 44 Eisele, M. and Burchard, W., manuscript in preparation
- 45 Huber, K. and Burchard, W. *Polymer*, in press
- 46 Dautzenberg, H. *Faserforsch. Textiltech.* 1970, **21**, 117
- 47 Dautzenberg, H. *Faserforsch. Textiltech.* 1970, **21**, 341